Relationship between electron-LO phonon and electron-light interaction in quantum dots

Nikola Prodanović,[*] Zoran Ikonić, Dragan Indjin, and Paul Harrison

Institute of Microwaves and Photonics, School of Electronic and Electrical Engineering, University of Leeds,
Woodhouse Lane, Leeds LS2 9JT, United Kingdom
(Received 23 February 2012; published 16 May 2012)

The relationship between the Frölich electron-LO phonon interaction and the electron-light interaction in the conduction band of quantum dots (QDs) based on polar semiconductors is investigated and used to parametrize the intersublevel polaron lifetime. Based on this, the ratio of the optical gain cross section and nonradiative lifetime is described in terms of the QD geometrical and compositional parameters, which is important for possible intraband lasing transitions in QDs.

PACS number(s): 78.67.Hc, 71.38.−k, 73.21.La

I. INTRODUCTION

In the last two decades, quantum dots have attracted considerable attention as potential candidates for improved lasing properties compared to their quantum well counterparts. The modified density of states due to the 3D quantum confinement increases the efficiency of lasing in comparison to the standard 1D confined structures, i.e., the quantum wells.[1,2] Experimental evidence that the system with truly discrete states should have a lower threshold current comes from the extremely low threshold currents observed in quantum-well-based quantum cascade lasers in the strong magnetic field.[3,4]

In Refs. 5 and 6 it was suggested that the dominant transition observed in the PL spectra is the transition between *s*-like and *p*-like states, which was based on numerical calculation of electronic states and optical matrix elements within the dipole approximation. There have been several reports on the observed intraband photoluminscence based on the *s-p*-like transitions in the quantum dot cascades.[5–7] Room temperature intraband photoluminiscence was observed in Ref. 8. However, lasing has not yet been observed.

Several theoretical proposals have been made for an intersublevel quantum dot cascade laser. They are either 2-level systems utilizing the *s-p*-like resonant transition for lasing[9–11] or 3-level systems[12] with the lasing transition between higher excited states in the quantum dots (QDs). The resonant *s-p*-like transition might be used for lasing in future designs of the QD intersublevel emitter. If not, we will here restrict considerations to this transition and the derived theory can be applied to other cases with a few modifications.

This resonant *s-p*-like transition requires a detailed investigation in terms of the radiative and nonradiative transition strengths. In order to obtain lasing, the strength of the radiative transition has to overcome population inversion losses due to nonradiative transitions. Therefore, the theoretical description of radiative and nonradiative relaxation processes is crucial, and it would be convenient to provide a theoretical insight which incorporates both nonradiative and radiative transitions.

The dipole approximation of the electron-radiation coupling has been widely accepted and used for the absorption and emission processes in various semiconductor nanostructures. The dipole approximation assumes that the light wavelength is substantially larger than the dot size, and therefore the electromagnetic field can be considered as spatially constant.

On the other hand the main source of nonradiative transitions comes from the electron-phonon coupling. Phonons behave as waves in the same manner as photons, and their second quantization is performed analogously.

The dominant electron-phonon interaction is Frölich interaction of electrons and longitudinal optical (LO) phonons. The Frölich interaction can be viewed as interaction of an electron and electromagnetic wave induced by dipole-like LO phonon vibrations. This sets up an analogy between the electron-phonon and the electron-photon interactions. The fundamental difference is that wave vectors of the relevant phonons are larger than those of photons and the dipole approximation does not hold for phonons.

Detailed theoretical predictions on the key nonradiative relaxation processes in the QD structures caused by Frölich interaction have evolved, relying on an increasing amount of available experimental data. First, it was thought that due to the discrete nature of the electronic structure and the nearly constant energy of LO phonons, the so-called phonon bottleneck would occur.[13] However, a great amount of experimental data showed the absence of this effect.[14,15]

Magneto-optical experiments in Refs. 16 and 17 showed that QDs behave like complex condensed matter systems where electrons and phonons interact strongly via polar Frölich coupling, thus forming quasiparticles, so-called polarons. Therefore, the simple picture of weak electron-phonon interaction was not appropriate.[18,19] The most prominent theoretical justification for a short lifetime of excited carriers in QDs has been presented in Refs. 15 and 20, where the lattice anharmonicity perturbation enables the energy exchange between different polaron modes, thus enabling relaxation toward the thermodynamical equilibrium.

The electron-phonon interaction remains the fundamental factor governing excited carrier nonradiative relaxation in QDs. The main aim of this work is to develop a simple model to establish a relationship between the radiative and the nonradiative transition strengths of carriers in QDs. The basis for it is a similar physical electromagnetic interaction between electrons and phonons, and electrons and photons. We will elaborate the relationship between these two interactions, and a short review of finite polaron lifetime theory will follow together with a model for optical gain and absorption coefficients. The model will then be used to derive important conclusions on the geometrical and compositional optimization of QDs as

possible active media. We will also underline the important role of state-of-the-art postgrowth fabrication modifications of QDs such as rapid thermal annealing[21] or quantum rod elongation[22,23] in future optimizations.

II. THE RELATIONSHIP

Since we are intrested only in s-p-like resonant coupling we introduce a reduction of the one-electron subspace into only the ground and the first excited electron states. Those electronic states will be further labeled with $|\psi_a\rangle$ and $|\psi_b\rangle$, or shortly $|a\rangle$ and $|b\rangle$, with energies E_a and E_b.

In this two-level system, the most important parameter regarding the electron-light interaction in dipole approximation is coordinate matrix element $\mathcal{R}_{ab} = \int d^3r \psi^{(a)*}(r)\hat{r}\psi^{(b)}(r)$ and will be referred to as a "dipole coupling vector." On the other hand, the same parameter for the Frölich interaction of the electron with the LO phonon mode with wave vector k is $\mathcal{H}_{ab}^{k} = \int d^3r \psi^{(a)*} \frac{e^{ik\cdot r}}{k} \psi^{(b)}$ and will be referred to as a "Frölich coupling function" (FCF) on wave vector k. The main aim here is to find a relationship between the dipole coupling vector $\mathcal{R}_{ab}$ and Frölich coupling function $\mathcal{H}_{ab}^{k}$.

In quantum dots, due to confinement, the Frölich coupling function falls rapidly to zero even for relatively small values of wave vector k. It behaves as a distribution function with p-orbital-like shape with the maximum value in the limit $k \rightarrow 0$. With the aim of estimating this value, one has to expand the expression for the Frölich coupling function as

$$
\begin{aligned}
\mathcal{H}_{ab}^{k} &= \int d^3r \psi^{(a)*} \frac{\cos k\cdot r}{k} \psi^{(b)} + i \int d^3r \psi^{(a)*} \frac{\sin k\cdot r}{k} \psi^{(b)} \\
&= \frac{1}{k} \int d^3r \psi^{(a)*} \psi^{(b)} + i e_k \cdot \int d^3r \psi^{(a)*} r \psi^{(b)} \\
&\quad - \frac{k}{2} \int d^3r \psi^{(a)*} (e_k \cdot r)^2 \psi^{(b)} \\
&\quad - i \frac{k^2}{6} \int d^3r \psi^{(a)*} (e_k \cdot r)^3 \psi^{(b)} + \cdots,
\end{aligned}
\tag{1}
$$

where the second equation represents the Taylor series of sine and cosine functions, and $e_k = \frac{k}{k}$.

Given that electronic states $|\psi_a\rangle$ and $|\psi_b\rangle$ are states with a dominant optical transition—i.e., the intensity of the dipole

coupling vector between these two states, $\mathcal{R}_{ab}$, is significant—then, in most cases, one concludes that states $\psi^{(a)}$ and $\psi^{(b)}$ have well-defined and opposite parity. Therefore, in such a case, the first term in Eq. (1) vanishes and one gets

$$
\mathcal{H}_{ab}^{k} = i\left(e_k \cdot \mathcal{R}_{ab} - \frac{k^2}{6} \int d^3r \psi^{(a)*}(e_k \cdot r)^3 \psi^{(b)} + \cdots \right).
\tag{2}
$$

In the limit $k \rightarrow 0$ expression (2) becomes

$$
\mathcal{H}_{ab}^{k} = e_k \cdot \mathcal{R}_{ab}.
\tag{3}
$$

Hence, the maximum of the scalar field $\mathcal{H}_{ab}^{k}$ is proportional to the intensity of the dipole coupling vector, and is at $k \rightarrow 0$.

It should be pointed that the FCF is singular at $k = 0$, and also the vector k does not have a defined direction, and therefore the expression $e_k \cdot \mathcal{R}_{ab}$ is not defined. However, the factor $e_k \cdot \mathcal{R}_{ab}$ indicates that even for small k the distribution $\mathcal{H}_{ab}^{k}$ has a strongly anisotropic behavior. For k pointing in the direction of the dipole coupling vector, the FCF exhibits the weakest negative slope. This slope is increasing with increasing angle between k and the FCF and decays rapidly to zero when k becomes almost perpendicular to the dipole coupling vector. In the limit where k is exactly perpendicular, the FCF is zero. All these features prove that the FCF has a p-orbital-like shape. This was indeed expected, since the FCF is essentially a Fourier transform of an even function.

One can demonstrate these statements by taking a simple example of a hard-wall cuboidal quantum dot where it is possible to calculate analytically $\mathcal{H}_{12}^{k}$ between the ground and the first excited state. The results for the quantum box of height 20 nm and square basis side of 15 nm are presented in Fig. 1(a) in the k_x-k_z plane without losing generality. The FCF behaves in the same way in the direction k_x as in k_y, for a square base case.

Therefore, we can model the Frölich coupling function by a bell-shaped distribution function, with the maximal value at $k \rightarrow 0$ proportional to the intensity of the dipole coupling vector and multiplied by the $\frac{k_i}{k}$, where i denotes the direction
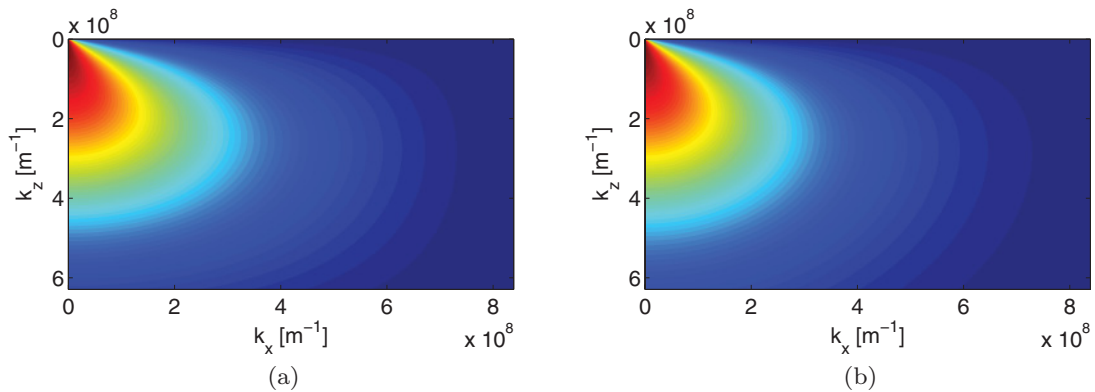

FIG. 1. (Color online) (a) The Frölich coupling function for a hard-wall box calculated in the k_x-k_z plane. The height of the dot is 20 nm and the square basis side is 15 nm. (b) The Frölich coupling function modeled by a Gaussian with fitted line width inversely proportional to the dot dimensions of the hard-walled QD. The whole Gaussian is multiplied by the cosine of the angle between k and k_z.

of the dipole coupling vector. This model gives

$$\left|\mathcal{H}_{\mathrm{ab}}^{\boldsymbol{k}}\right| = \left|\mathcal{R}_{\mathrm{ab}}\right| \frac{k_z}{\sqrt{k_x^2 + k_y^2 + k_z^2}} \mathcal{I}(\boldsymbol{k}), \tag{4}$$

where $\mathcal{I}(\boldsymbol{k})$ is the anisotropic distribution function with maximum $\mathcal{I}(0) = 1$. Therefore, we have parametrized the FCF via two factors. One is the dipole coupling vector $\mathcal{R}_{\mathrm{ab}}$ which is a well-known spectroscopic quantity, and the second is the distribution function with the property $\mathcal{I}(0) = 1$. All details of the quantum dot are hidden in the width and line shape of this function. We will show later that the most important quantity regarding nonradiative relaxation is the integral of the squared absolute value of distribution function. This is why the exact line shape has a limited significance. On the other hand, we will show that widths of the distribution functions are closely related to the size of the quantum dot in the corresponding direction.

III. POLARON STATES

Electrons and LO phonons are in a strong-coupling regime in the polar semiconductor quantum dots.[16,24] The full Hamiltonian to be considered accounts for the Frölich coupling between electrons and LO phonons, i.e.,

$$H = H_{\mathrm{e}} + H_{\mathrm{ph}} + \sqrt{\frac{e^2 \hbar \omega_{\mathrm{LO}}}{2V} \left(\frac{1}{\epsilon_\infty} - \frac{1}{\epsilon_{st}}\right)}$$
$$\times \sum_{ij\boldsymbol{k}} \mathcal{H}_{ij}^{\boldsymbol{k}} \hat{a}_i^+ \hat{a}_j (\hat{b}_{\boldsymbol{k}} + \hat{b}_{-\boldsymbol{k}}^+), \tag{5}$$

where H_{e} is the electronic part of the Hamiltonian, H_{ph} is the phonon part of the Hamiltonian, $\hat{b}_{\boldsymbol{k}}$ and $\hat{b}_{\boldsymbol{k}}^+$ are phonon annihilation and creation operators, and $\hat{a}_i$ and $\hat{a}_j^+$ are the corresponding operators for electrons. It has been argued that one has to diagonalize this full Hamiltonian in order to obtain agreement with results obtained in magneto-optical experiments.[15–17]

The diagonalization procedure from Ref. 19 has been adopted here. The Hamiltonian, Eq. (5), commutes with the electron number operator $\hat{N}$ and therefore can be solved in each subspace for a constant number of electrons. Therefore, the one-electron limitation is introduced here together with the two-level system explained above.

The eigenstates of the trivial case of the Hamiltonian without electron-phonon interaction is a simple uncorrelated eigenbasis formed by the direct product of a pure electronic eigenstates and pure phonon eigenstates. When it comes to the full Hamiltonian, as has been proved in Refs. 17 and 19, only a finite number of LO modes couples with a finite number of electronic states in the nondispersive phonon modes approximation. For two-level electronic systems only three LO modes are considered. Their further orthonormalization[25] and proper unitary rotation give three new modes which are coupled to a two-level system with one electron. Only one mode couples the s-p resonant transition to the classical emission or absorption of one phonon and will be denoted as B_1. The second mode couples the s-p resonant transition with the self-translation which gives rise to the Franck-Condon factors.[19] It will be denoted as B_2^γ where the parameter γ

represents translation. The third mode is properly translated so it does not couple to the resonant s-p transition in the one-electron case and can be omitted from further consideration.

Further space reduction was obtained in Ref. 19 by introducing the rotating wave approximation, by choosing only the coupling states differing by the detunings $\delta_\pm = E_b - E_a \pm \hbar \omega_{\mathrm{LO}}$. The first state has the electron in state b and "certain phonon configuration." The second state has the electron in state a and the same phonon configuration, with only one additional phonon in mode B_1 and "translated" mode B_2^γ with the same occupation number. The relationship between these translated and initial modes is determined by general Franck-Condon factors. By neglecting the polaronic shift terms, it is possible to obtain approximate analytical solution of any such 2×2 Hamiltonian. Thus, the basis considered is

$$\left|2'\right\rangle = \left|b; n_1^0; n_2^\gamma\right\rangle, \quad \left|3'\right\rangle = \left|a; n_1^0 + 1; n_2^0\right\rangle,$$

where $n_1 = n_2 = 0$. We additionally take two adjacent states into account, namely the ground state a with zero phonons (i.e., uncorrelated ground state) and its coupling state b with one phonon in mode B_1 and the "translated" mode B_2^γ with the same occupation number:

$$\left|1'\right\rangle = \left|a; n_1^0; n_2^0\right\rangle, \quad \left|4'\right\rangle = \left|b; n_1^0 + 1; n_2^\gamma\right\rangle.$$

The superscript at the phonon modes denotes translation of the mode from the bulk one. Enumeration of the basis states is made to order the states according to their increasing energy; i.e., we consider the case where the detuning is $\delta_- < 0$.

The solution of this model is also given in Ref. 19 and it reads

$$\left|1\right\rangle = \sqrt{\frac{1}{2}\left(1 - \frac{\delta_+}{R_+}\right)}\left|4'\right\rangle + \sqrt{\frac{1}{2}\left(1 + \frac{\delta_+}{R_+}\right)}\left|1'\right\rangle,$$

$$\left|2\right\rangle = \sqrt{\frac{1}{2}\left(1 - \frac{\delta_-}{R_-}\right)}\left|2'\right\rangle - \sqrt{\frac{1}{2}\left(1 + \frac{\delta_-}{R_-}\right)}\left|3'\right\rangle,$$

$$\left|3\right\rangle = \sqrt{\frac{1}{2}\left(1 + \frac{\delta_-}{R_-}\right)}\left|2'\right\rangle + \sqrt{\frac{1}{2}\left(1 - \frac{\delta_-}{R_-}\right)}\left|3'\right\rangle,$$

$$\left|4\right\rangle = \sqrt{\frac{1}{2}\left(1 + \frac{\delta_+}{R_+}\right)}\left|4'\right\rangle - \sqrt{\frac{1}{2}\left(1 - \frac{\delta_+}{R_+}\right)}\left|1'\right\rangle,$$

where $R_+ = \sqrt{\delta_+^2 + 4|F_n^\gamma C_{\mathrm{ab}}|^2}$ and $R_- = \sqrt{\delta_-^2 + 4|F_n^\gamma C_{\mathrm{ab}}|^2}$ are the Rabi splittings, while $F_n^\gamma = \langle n|n\rangle_\gamma$ is the Franck-Condon factor and $C_{\mathrm{ab}} = \sum_{\boldsymbol{q}} |M_{\mathrm{ab}}(\boldsymbol{q})|^2$ is a normalization constant used to normalize the mode B_1. If one assumes zero energy of the state $\left|1'\right\rangle$ the eigenenergies of this polaron model are

$$E_1 = \tfrac{1}{2}(\delta_+ - R_+), \quad E_2 = \tfrac{1}{2}(\delta_+ - R_-),$$
$$E_3 = \tfrac{1}{2}(\delta_+ + R_-), \quad E_4 = \tfrac{1}{2}(\delta_+ + R_+).$$

In conclusion to this section, the most important quantity, directly responsible for formation of the coherent polaron modes, is the normalization constant C_{ab}. In terms of the FCF this normalization constant reads

$$C_{\mathrm{ab}} = \frac{e^2 \hbar \omega_{\mathrm{LO}}}{16\pi^3}\left(\frac{1}{\epsilon_\infty} - \frac{1}{\epsilon_{st}}\right)\int d^3\boldsymbol{k} \left|\mathcal{H}_{\mathrm{ab}}^{\boldsymbol{k}}\right|^2 \tag{6}$$

and will be further referred to as the Frölich coupling constant. By using the relation (4), the Frölich coupling constant becomes

$$|C_{ab}|^2 = \frac{e^2 \hbar \omega_{LO}}{16\pi^3} \left(\frac{1}{\epsilon_\infty} - \frac{1}{\epsilon_{st}} \right) |\mathcal{R}_{ab}|^2 S, \qquad (7)$$

where

$$S = \int d^3 \mathbf{k} \frac{k_z^2}{k_x^2 + k_y^2 + k_z^2} \mathcal{I}^2(\mathbf{k}) \qquad (8)$$

will be further on referred to as the coupling integral constant.

We have deconstructed the Frölich coupling constant for any quantum dot via factors containing the dipole coupling vector and integrals of the distribution function. Due to this integral, the precise shape of this distribution function becomes unimportant, and only its linewidth remains as a crucial factor determining the value of the coupling integral constant S.

IV. INFLUENCE OF QD GEOMETRY AND COMPOSITION

In the following we give a quantitative description of the influence of the QD confinement on the value of expression (6). Consider first the distribution function. Anisotropy of this function stems from the dimensional anisotropy of the dot. Thus, for anisotropic QDs the linewidth of such a distribution function varies with the direction in $\mathbf{k}$ space.

The Frölich coupling function can be thought of as a Fourier transform of the product of wave functions in the ground and excited state divided by k. By varying the dot dimensions we can shrink or expand the envelope wave functions. This can be modeled by

$$\psi(x,y,z) \to \sqrt{\alpha_x \alpha_y \alpha_z} \psi(\alpha_x x, \alpha_y y, \alpha_z z). \qquad (9)$$

Using these scaled wave functions in the Frölich coupling function, and taking a particular direction, e.g., the "x" direction (i.e., setting $k_y = k_z = 0$), one concludes that the

FCF has the behavior

$$\mathcal{H}_{ab}(k_x,0,0) \to \frac{1}{\alpha_x} \mathcal{H}_{ab}\left(\frac{k_x}{\alpha_x}, 0, 0 \right). \qquad (10)$$

However, the prefactor $\frac{1}{\alpha_x}$ is already included in the scaling of the dipole coupling vector, and therefore only the scaling of the distribution function width has to be considered further. By increasing the dot size in the chosen direction one can decrease the distribution function width in that direction. However, this trend remains up to some minimal, critical size in a particular direction. Beyond this point, the envelope wave function does not shrink any further, but instead starts leaking outside the dot. In the hard-wall example, it is possible to use a Gaussian without a normalization prefactor as a distribution function. The results of such a model are presented in Fig. 1(a). The width of the Gaussian is inversely proportional to the dot extension in the corresponding direction. The modeling by the Gaussian curve is also the exact solution for a parabolic QD (see Appendix of Ref. 19).

For calculations with better accuracy we use an 8-band $\mathbf{k} \cdot \mathbf{p}$ method with strain effects included to calculate the Frölich coupling function and demonstrate its dependence on the dot size.[11,18,26,27] In Figs. 2(a) and 2(b) we present the calculated FCF for lens-shaped dots of height 8 nm, indium content 1, and radius 22 nm. The second dot is twice as high, 16 nm, and we note that FCF has accordingly shrunk twofold in this direction. The In content in the QD also affects the width of the distribution function. By decreasing the In content one decreases the QD potential well and the confinement. The wave functions then expand and the FCF consequently shrinks, and so does the distribution function. This is demonstrated in Figs. 3(a) and 3(b), where two geometrically identical QDs (cylinder shaped) have different In content, of 1 and 0.6, respectively. We note that FCF in Fig. 3(b) is slightly narrower than that in Fig. 3(a). It is expected that the maximal possible width of the distribution function in terms of QD depth occurs for the hard-wall QD, since it has infinite potential well. The opposite limit occurs in bulk, where the width is zero; i.e., the
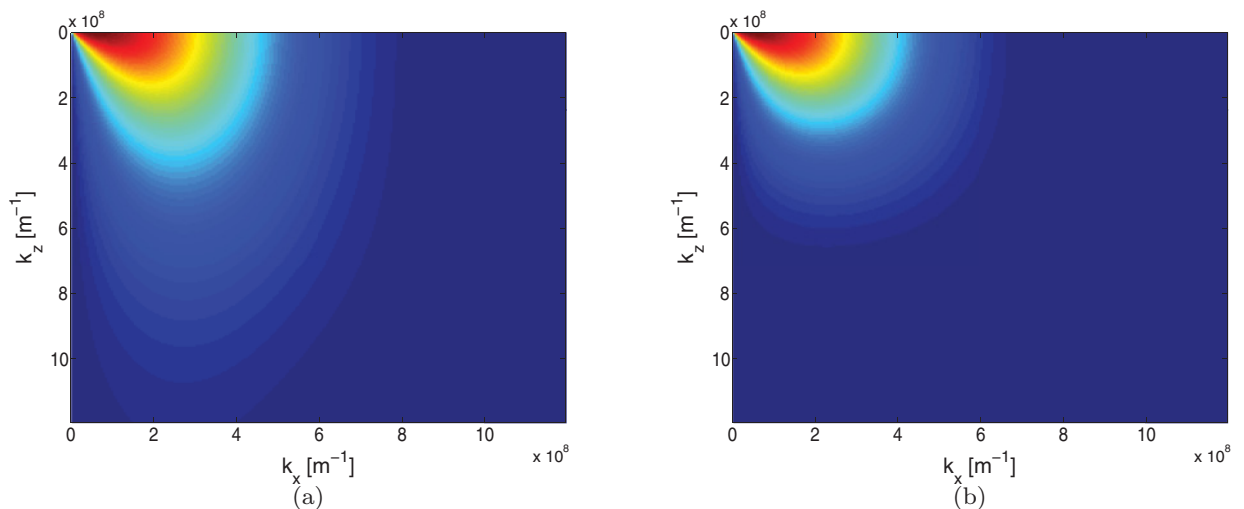

FIG. 2. (Color online) FCF for two different lens-shaped cylindrically symmetric QDs calculated in the k_x-k_z plane by the 8-band $\mathbf{k} \cdot \mathbf{p}$ method with strain effects included. Indium content in both dots is 1, radius is 22 nm, and their height is (a) 8 nm and (b) 16 nm.
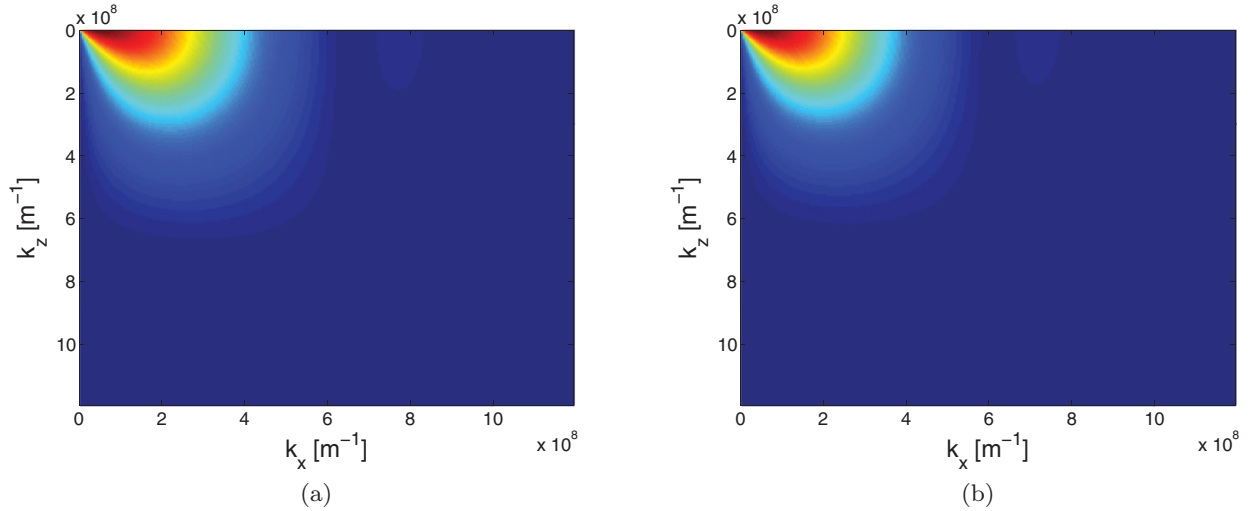
FIG. 3. (Color online) (a) FCF for two different cylinder-shaped QDs calculated in the k_x-k_z plane by the 8-band $\boldsymbol{k} \cdot \boldsymbol{p}$ method with strain effects included. Indium content in dots is (a) 1 and (b) 0.6, and their radius and height are 22 nm and 12 nm, respectively, in both cases.

wave function is a pure plane wave. It is difficult to predict a more accurate dependence of the width of the distribution function, but a monotonic behavior is expected between these two limits.

In summary, we have introduced four parameters: $\alpha_x, \alpha_y, \alpha_z$, and σ. The first three parameters measure the relative QD extension in a specified direction, and the parameter σ is an increasing function of the In content in the QD. By varying these geometrical parameters the distribution function evolves as

$$\mathcal{I}(k_x, k_y, k_z) \rightarrow \mathcal{I}\left(\frac{\alpha_x}{\sigma} k_x, \frac{\alpha_y}{\sigma} k_y, \frac{\alpha_z}{\sigma} k_z\right) \quad (11)$$

and consequently the coupling integral constant evolves as

$$S \rightarrow \int d^3 \boldsymbol{k} \frac{k_z^2}{k_x^2 + k_y^2 + k_z^2} \mathcal{I}\left(\frac{\alpha_x}{\sigma} k_x, \frac{\alpha_y}{\sigma} k_y, \frac{\alpha_z}{\sigma} k_z\right), \quad (12)$$

which gives

$$S \rightarrow \frac{\sigma^3}{\alpha_x \alpha_y \alpha_z} \int d^3 \boldsymbol{k} \frac{k_z^2}{\left(\frac{\alpha_z}{\alpha_x}\right)^2 k_x^2 + \left(\frac{\alpha_z}{\alpha_y}\right)^2 k_y^2 + k_z^2} \mathcal{I}(\boldsymbol{k})$$

$$= \frac{\sigma^3}{\alpha_x \alpha_y \alpha_z} S'. \quad (13)$$

Equation (13) describes the variation of the coupling integral constant in terms of quantum dot geometric and composition parameters. The largest contribution comes from the prefactor. Coupling integral constant S is slightly different from S'; i.e., it differs only by the "cosine part." In the case of an isotropic enlargement of the QD size, the "cosine part" in the integrals remains unchanged and therefore so do the constants S and S'.

V. LIGHT ABSORPTION AND STIMULATED EMISSION

The polaron ground state is $|1\rangle$ with the dominant component being the electron ground state. In the case of $\delta_- < 0$, the first excited polaron state is $|2\rangle$. As expected, the dominant component of that state is the first excited electron state,

which enables efficient optical excitation of that polaron state from the ground state. Therefore, when dealing with optical excitation, we will omit the polaronic nature of the carriers in QDs and will derive expressions for the quantities of interest with pure electronic notation. Later, we will only replace the electronic notation with the corresponding polaronic notation. Let the system be described semiclassically, with particular interest in estimating the transition rate between the lower state $|a\rangle$ with energy E_a and the higher state $|b\rangle$ with energy E_b. Within this semiclassical approach, Fermi's golden rule transition rate can be used to find the coefficients of absorption and stimulated emission gain in the active medium. The optical cross section gives the absorption line and gain when multiplied by the population difference. With the "$-e\hat{\boldsymbol{r}} \cdot \boldsymbol{E}$" interaction the expression for optical cross section reads[28]

$$\sigma_{ab}^{\boldsymbol{\varepsilon}}(\omega) = \frac{4\pi |e|^2 \omega}{\bar{n} \varepsilon_0 c m_0^2} |\boldsymbol{\mathcal{R}}_{ab} \cdot \boldsymbol{\varepsilon}|^2 g(E_b - E_a \mp \hbar\omega), \quad (14)$$

where $g(E_b - E_a \mp \hbar\omega)$ is the normalized distribution function (e.g., Gaussian), recovering the inhomogeneous broadening due to the size inhomogeneity of the quantum dot ensemble and $\boldsymbol{\varepsilon}$ is the light polarization unit vector. Constants e, m_0, $\bar{n}$, and c are electron charge and mass, refractive index of the quantum dot, and speed of light. The sign "$-$" corresponds to absorption and "$+$" to emission.

VI. NONRADIATIVE POLARON LIFETIME

After excitation, the relaxation of nonequilibrium polarons is enabled by anharmonic perturbation of the crystal. So far, this has been the most reliable theoretical explanation of the finite excited carrier lifetime proposed in Ref. 29. This potential acts only on the phonon factor in the polaron state. Besides the zero-phonon component in the excited polaron state, there is also a one-phonon component responsible for nonradiative relaxation of the excited polaron due to crystal anharmonicity potential. Therefore, the nonradiative decay rate has to be proportional to the absolute squared value of

the weights of the relevant components:

$$\Gamma(E_i) = \frac{1}{4}\Gamma_{\mathrm{ph}}(E_i)\left(1 + \frac{\delta_+}{R_+}\right)\left(1 + \frac{\delta_-}{R_-}\right). \quad (15)$$

The quantity $\Gamma_{\mathrm{ph}}(E_i)$ represents the bare decay rate of phonons which would have polaron energies driven by anharmonicity potential:

$$\Gamma_{\mathrm{ph}}(E_i) = \frac{2\pi}{\hbar}\sum_j |\langle j|V_a|3'\rangle|^2. \quad (16)$$

The summation is performed over all possible decay channels of mode B_1 with one phonon. Detailed discussion on decay channels and the derivation of analytical expression for $\Gamma_{\mathrm{ph}}(E_i)$ can be found in Ref. 29.

It was pointed out in Ref. 20 that a strong inhibition of this mechanism occurs at lower values of the energy splitting between the electronic ground and excited states. In other words, the squared detuning δ_-^2 becomes significantly larger than the squared Frölich coupling constant, leading to a simplified linearized ratio of detuning and Rabi splitting:

$$1 + \frac{\delta_-}{R_-} \approx 2\frac{|F_n^\gamma C_{ab}|^2}{\delta_-^2}. \quad (17)$$

Furthermore, by using an additional approximation $\frac{\delta_+}{R_+} \approx 1$ and $F_n^\gamma \approx 1$, which holds for small values of the parameter γ, one can write

$$\Gamma(E_i) = \Gamma_{\mathrm{ph}}(E_i)\frac{|C_{ab}|^2}{\delta_-^2}. \quad (18)$$

Therefore, the Frölich coupling constant is directly proportional to the lifetime of the excited carrier in the quantum dot.

VII. LASING EFFICIENCY

In order to consider a transition as a possible lasing transition, both the radiative and nonradiative lifetimes are important. The longer the nonradiative lifetime, the higher is the likelihood of photon emission. Thus, we define a figure of merit for such a transition as the ratio of the optical cross section and the nonradiative transition rate for the light polarized along the dipole coupling vector $K_{ab}(\omega) = \frac{\sigma_{ab}(\omega)}{\Gamma(E_i)}$. By using Eqs. (14) and (18) the lasing figure of merit becomes

$$K_{ab}(\omega) = \frac{64\pi^4 g(E_i \mp \hbar\omega)}{\bar{n}\varepsilon_0 c m_0^2 \hbar^2 \omega_{\mathrm{LO}}\left(\frac{1}{\epsilon_\infty} - \frac{1}{\epsilon_{st}}\right)}\frac{\delta_-^2}{S(E_i)}\frac{E_i}{\Gamma_{\mathrm{ph}}}. \quad (19)$$

The inhomogeneous broadening $g(E_i \mp \hbar\omega)$ clearly affects this laser efficiency coefficient, via the optical cross section. Increasing the inhomogeneous broadening width will decrease the laser efficiency for a specific frequency of light. The ratio $\frac{E_i}{\Gamma_{\mathrm{ph}}}$ is proportional to $\frac{1}{E_i^n}$, where n is an integer depending on the active disintegration channel. A detailed discussion on this subject is presented in Ref. 29, but the general conclusion is that a decrease of polaron s-p-like splitting E_i will lead to improved lasing efficiency. Dot enlargement and a reduced In content also lead to a decrease of the quantity S, as explained in the previous section. Furthermore, the squared detuning δ_-^2 then increases and leads to improved lasing efficiency.

It is clear now that novel postfabrication techniques such as rapid thermal annealing[21] or quantum rod elongation[22,23] could produce structures with higher lasing efficiency coefficient. One can enlarge the dot, or reduce the In content by using those techniques. In Ref. 20, it has been demonstrated that the nonradiative polaron lifetime is increased by rapid thermal annealing. However, we have shown here that this does not affect adversely the radiative lifetime, thus increasing the overall figure of merit (19).

VIII. CONCLUSION

In summary, in an ideal symmetric case, the FCF was parametrized with the dipole coupling vector (optical matrix element) and the distribution function whose widths were related to geometrical and compositional properties of the quantum dot. Based on such parametrization we have established a direct relationship between nonradiative lifetime and optical gain for a possible lasing transition in self-assembled quantum dots based on polar semiconductors. This was further used to derive an appropriate figure of merit for the lasing transition, which depends directly on geometrical parameters of the dot and on the level spacing. Enlargement of the quantum dot and reduction of In content in the dot lead to a higher figure of merit and both can be achieved by rapid thermal annealing. Novel structures such as quantum rods can be elongated in the growth direction, leading to a higher figure of merit.

Certainly, going to the extreme with such tailoring of dot structure will eventually bring in additional effects which may deteriorate lasing, and were not here accounted for. As the level spacing decreases, the thermal backfilling sets in, reducing the population inversion. Furthermore, the difficulty of selective electron injection into the excited state becomes more prominent as it gets close to the ground state.

Therefore, one has to solve the full system of rate equations in order to model the quantum-dot-based quantum cascade laser properly. The aim of this work was primarily to study the radiative versus nonradiative lifetimes, and to describe this problem via the minimum possible number of parameters. We also aimed to simplify the description of the Frölich coupling between confined electron states in the QD conduction band. The important parameters in this coupling have been deconstructed as much as possible to experimentally measurable spectroscopic quantities such as level spacing and dipole coupling vector.

ACKNOWLEDGMENTS

*elnpr@leeds.ac.uk

[1] Y. Arakawa and H. Sakaki, Appl. Phys. Lett. **40**, 939 (1982).

[2] N. N. Ledentsov, M. Grundmann, F. Heinrichsdorff, D. Bimberg, V. M. Ustinov, A. E. Zhukov, M. V. Maximov, Z. I. Alferov, and J. A. Lott, IEEE J. Sel. Top. Quantum Electron. **6**, 439 (2000).

[3] G. Scalari, S. Blaser, J. Faist, H. Beere, E. Linfield, D. Ritchie, and G. Davies, Phys. Rev. Lett. **93**, 237403 (2004).

[4] A. Wade, G. Fedorov, D. Smirnov, S. Kumar, B. S. Williams, Q. Hu, and J. L. Reno, Nature Photonics **3**, 41 (2009).

[5] N. Ulbrich, J. Bauer, G. Scarpa, R. Boy, D. Schuh, G. Abstreiter, S. Schmult, and W. Wegscheider, Appl. Phys. Lett. **83**, 1530 (2003).

[6] C. Fischer, P. Bhattacharya, and P.-C. Yu, Electron. Lett. **39**, 1537 (2003).

[7] S. Anders, L. Rebohle, F. F. Schrey, W. Schrenk, K. Unterrainer, and G. Strasser, Appl. Phys. Lett. **82**, 3862 (2003).

[8] D. Wasserman, T. Ribaudo, S. A. Lyon, S. K. Lyo, and E. A. Shaner, Appl. Phys. Lett. **94**, 061101 (2009).

[9] C.-F. Hsu, J.-S. O, P. Zory, and D. Botez, IEEE J. Sel. Top. Quantum Electron. **6**, 491 (2000).

[10] V. M. Apalkov and T. Chakraborty, Appl. Phys. Lett. **78**, 1820 (2001).

[11] N. Vukmirovic, D. Indjin, Z. Ikonic, and P. Harrison, IEEE Photonics Technol. Lett. **20**, 129 (2008).

[12] I. A. Dmitriev and R. A. Suris, Phys. Status Solidi A **202**, 987 (2005).

[13] U. Bockelman and G. Bastard, Phys. Rev. B **42**, 8947 (1990).

[14] S. Sauvage, P. Boucaud, R. P. S. M. Lobo, F. Bras, G. Fishman, R. Prazeres, F. Glotin, J. M. Ortega, and J.-M. Gérard, Phys. Rev. Lett. **88**, 177402 (2002).

[15] E. A. Zibik, L. R. Wilson, R. P. Green, G. Bastard, R. Ferreira, P. J. Phillips, D. A. Carder, J.-P. R. Wells, J. W. Cockburn, M. S. Skolnick, M. J. Steer, and M. Hopkinson, Phys. Rev. B **70**, 161305 (2004).

[16] S. Hameau, Y. Guldner, O. Verzelen, R. Ferreira, G. Bastard, J. Zeman, A. Lemaître, and J. M. Gérard, Phys. Rev. Lett. **83**, 4152 (1999).

[17] S. Hameau, J. N. Isaia, Y. Guldner, E. Deleporte, O. Verzelen, R. Ferreira, G. Bastard, J. Zeman, and J. M. Gérard, Phys. Rev. B **65**, 085316 (2002).

[18] N. Vukmirović, Z. Ikonić, D. Indjin, and P. Harrison, Phys. Rev. B **76**, 245313 (2007).

[19] T. Stauber, R. Zimmermann, and H. Castella, Phys. Rev. B **62**, 7336 (2000).

[20] E. A. Zibik, T. Grange, B. A. Carpenter, N. E. Porter, R. Ferreira, G. Bastard, D. Stehr, S. Winnerl, M. Helm, H. Y. Liu, M. S. Skolnick, and L. R. Wilson, Nature Mater. **8**, 803 (2009).

[21] S. Fafard, Z. R. Wasilewski, C. N. Allen, D. Picard, M. Spanner, J. P. McCaffrey, and P. G. Piva, Phys. Rev. B **59**, 15368 (1999).

[22] L. Li, G. Patriarche, N. Chauvin, P. Ridha, M. Rossetti, J. Andrzejewski, G. Sek, J. Misiewicz, and A. Fiore, IEEE J. Sel. Top. Quantum Electron. **14**, 1204 (2008).

[23] J. He, H. J. Krenner, C. Pryor, J. P. Zhang, Y. Wu, D. G. Allen, C. M. Morris, M. S. Sherwin, and P. M. Petroff, Nano Lett. **7**, 802 (2007).

[24] T. Inoshita and H. Sakaki, Phys. Rev. B **56**, R4355 (1997).

[25] T. Stauber and R. Zimmermann, Phys. Rev. B **73**, 115303 (2006).

[26] N. Prodanović, N. Vukmirović, D. Indjin, Z. Ikonić, and P. Harrison, J. Phys.: Conf. Ser. **242**, 012012 (2010).

[27] N. Vukmirović, D. Indjin, V. D. Jovanović, Z. Ikonić, and P. Harrison, Phys. Rev. B **72**, 075356 (2005).

[28] W. E. Lamb, R. R. Schlicher, and M. O. Scully, Phys. Rev. A **36**, 2763 (1987).

[29] T. Grange, R. Ferreira, and G. Bastard, Phys. Rev. B **76**, 241304 (2007).